WIND TUNNEL STUDY AND DNS OF STABLE BOUNDARY LAYERS AND CONVECTIVE BOUNDARY LAYERS IN THE ATMOSPHERE

Yuji Ohya
Research Institute for Applied Mechanics, Kyushu University
Kasuga 816-8580, Japan

Takanori Uchida
Research Institute for Applied Mechanics, Kyushu University
Kasuga 816-8580, Japan

ABSTRACT

The atmospheric boundary layers with a wide range of stability are simulated experimentally using a thermally stratified wind tunnel and numerically by DNS. The turbulence structure and flow characteristics of stratified boundary layers under both stable and unstable conditions are investigated. For stable boundary layers (SBL), attention is focused on the buoyancy effects on stratified turbulent flows with strong stability. Wave-like motions driven by buoyancy and waves due to the Kelvin-Helmholtz instability can be observed in the lower part of boundary layers with very strong stability. Simulations on the convective boundary layers (CBL), capped by a strong temperature inversion and affected by surface shear, are also carried out. The comparison of the wind tunnel data and DNS results with those of atmospheric and water tank studies of CBL shows the crucial dependence of the turbulence statistics in the upper part of the layer on the strength of inversion layer, as well as the modification of the CBL turbulence regime by the surface shear.

INTRODUCTION

Turbulence within the atmospheric boundary layer (ABL) is generated and maintained by two forces: wind shear and buoyancy. Wind shear dominates the neutral and most of the stable ABL (Stable Boundary Layers, SBL), while buoyancy dominates the convective ABL (Convective Boundary Layers, CBL). Depending on the dominant forcing mechanism, the ABL flow patterns and turbulence statistics can be quite different, as pointed out by numerous studies, for example, Arya(1982), Caughey (1984), Stull (1988) and Wyngaard (1992).

Recently, Mahrt et al. (1998) and Mahrt (1999) have discussed various features of different stability regimes of SBL, in particular, focusing on the very stable case, and pointed out that similarity theory and the traditional concept of a boundary layer break down for the very stable case. For laboratory experiments on the ABL with a wide variety of stratification, a thermally stratified wind tunnel, which can produce various stratified flows in the test section, is a very useful facility to simulate the ABL flows (Meroney and Melbourne 1992, Ohya et al. 1996, Fedorovich et al. 1996). For SBL laboratory studies in the past, the stably stratified flows obtained have been limited within relatively weak stabilities (Arya 1975, Komori et al. 1983), thus the experimental results with a wide range of stability including very strong stability are very few (Ohya, et al. 1997). Therefore, the turbulence structures and transport processes in the strongly stable boundary layers still remain unclear.

For the atmospheric CBL, a number of CBL laboratory studies have been reported so far (for example, Willis and Deardorff 1974, Fedorovich et al. 1996), there are, however, hardly any study which could successfully simulate a capping inversion aloft and surface shear simultaneously, due to the limited capability of those facilities. Therefore, the detailed mechanisms of the penetration of thermals or plumes into the inversion layer and of the entrainment of the fresh air aloft into the mixed layer have not yet been fully clarified.

In the present study, we have developed the simulation methods for SBL including strong stability cases and for CBL with a strong capping inversion aloft, by using a specially designed thermally stratified wind tunnel. We have investigated turbulence structures and transport processes of SBL and CBL simulated in the test section, comparing the results to those of the field and other laboratory studies.

In parallel with wind tunnel experiments, to understand the turbulence features and fluid dynamics of the SBL and CBL in detail, we have also performed numerical simulations of both SBL and CBL under the boundary conditions similar to those in the wind tunnel experiments. The numerical studies based on a finite-difference method (FDM) are direct Navier-Stokes simulations without any turbulence model and accordingly the Reynolds numbers are relatively lower than those in wind tunnel experiments. However, comparing the computational results with the experimental ones, we can

have better understanding of the atmospheric SBL and CBL.

THERMALLY STRATIFIED WIND TUNNEL AND EXPERIMENTAL METHOD

Experiments were performed in a thermally stratified wind tunnel of Kyushu University (Ohya et al. 1996). The wind tunnel is of a suction type and has a 1.5m wide, 1.2m high, 13.5m long, rectangular test section. Designed to produce thermally stratified flows, the tunnel is equipped with two independent temperature systems which consist of an air-flow heating unit (AHU) and a floor temperature controlling unit (FTCU). Using the AHU and FTCU, a wide range of thermal stratification can be generated with a wind speed in the range of 0.2-2.0m/s. The experimental arrangements for SBL and CBL simulations are shown in Figures 1 and 8, respectively. The boundary layer was artificially tripped by a two-dimensional (2D) block with a height of 5 cm at the entrance of the test section and by chain roughness placed over the floor for SBL experiment (for CBL experiment, there is no chain roughness). The velocity and temperature fluctuations were measured simultaneously using a sensor system of an x-type hot-wire and a cold-wire at a downwind position, where the boundary layer is fully developed. Flow visualization of the simulated SBL and CBL was also carried out by a smoke-wire device placed inside the test section and a smoke generator unit placed at the inlet of the AHU.

NUMERICAL SIMULATION

Direct numerical simulations of stratified boundary layers under various stability conditions were also made by a finite-difference method without any turbulence model. The calculation domains are 9m long (x-direction), 1m wide (y), 1m high (z) for SBL and 9m long (x), 1.6m wide (y), 1m high (z) for CBL. A Cartesian grid system consists of uniform horizontal grids and vertical non-uniform grids concentrated toward the ground. The number of grid points in the x, y and z-directions are 601x101x91 for SBL and 401x161x81 for CBL. Under the Boussinesq approximation, the governing equations consist of the Navier-Stokes, continuity and energy equations for 3D incompressible stratified flow. The boundary conditions are almost similar to those with the wind tunnel experiments except for the surface roughness by chain over the test section floor for SBL. The numerical method is a variant of a fractional-step method. For time advance, the Euler explicit method is used. All the spatial derivatives are approximated with second-order central differences on a staggered grid.

STABLE BOUNDARY LAYERS

Experimental and Computational Setup

A stably stratified flow is created by heating the wind tunnel airflow at around 40 - 50℃ and by cooling the test-section floor at around 10℃, as shown in Figure 1. The stratified turbulent boundary layers with freestream velocities, U_∞= 0.7-1.9 m/s, cover a range of stability from neutral to strongly stable.

As summarized in Table 1, the Reynolds number, Re_δ, (= $U_\infty \delta / \nu$), based on the boundary layer thickness, δ, ranges from $2x10^4$ to $5.3x10^4$ and the bulk Richardson number, Ri_δ (= $(g/\Theta_O) \cdot (\Theta_\infty - \Theta_S) \delta / U_\infty^2$), ranges from 0 to 1.17. Here, ν is the coefficient of kinematic viscosity, g, the acceleration due to gravity, Θ_O, the average absolute temperature over the whole boundary layer depth, Θ_s, the temperature of cooled floor, Θ_∞, the temperature of ambient air at δ, and $\Delta\Theta$, the difference of $\Theta_\infty - \Theta_S$. Measurements of turbulence quantities in the vertical direction were made at a distance of 9 m downstream from the 2D block. The computational data of a neutral and stratified flows are shown in Table 2. It should be noted that the Reynolds numbers are much lower than those of experiments.

Results

Table 1 shows the flow conditions for each experimental case (N1 - S8). The vertical profiles in Figures 2 and 3 are normalized by U_∞ and $(\Theta_\infty - \Theta_S)$, and shown with the normalized height z/δ. Stable stratification rapidly suppresses the fluctuations of streamwise velocity, u, and temperature, θ, as well as the vertical velocity fluctuation, w, as shown in Figure 2. These profiles display great differences in the lower half depth of the boundary layer, namely, the intensities of u fluctuation for the cases S5-S8 with strong stability approach zero as z/δ decreases from the middle of the boundary layer to the bottom. Momentum fluxes are also significantly decreased with increasing stability and become nearly zero in the lowest part of the boundary layer with strong stability (cases S6-S8), as shown in Figure 3a. For the computational result as shown in Figure 3b, the momentum flux profile of stratified flow is very similar to those of experiments with strong stability. The profiles of turbulence fluctuations and fluxes in Figures 2 and 3 with weak stability cases S1-S4 are similar to the results obtained in the wind tunnel experiments by Arya (1975) and Ohya, et al.(1997) and also similar to the observational results from Caughey et al. (1979) and Nieuwstadt (1984).

The vertical profiles of turbulence statistics exhibit different behavior in two distinct stability regimes of the stratified flows with weak stability (Ri_δ=0- 0.27) and those with strong stability (Ri_δ=0.4- 1.17), as shown in Figures 2 and 3. The two stability regimes of stratified flows clearly show different vertical profiles of the mean local gradient Richardson number Ri, separated by the critical Richardson number, Ri_{cr}, of about 0.25, as shown in Figure 4. As noted above, it is expected that Ri number can be an important scaling parameter for correlating turbulent quantities. However, for the regions near the bottom and top of the boundary layer, both turbulence quantities and Ri greatly change in magnitude, suggesting a condition far from local equilibrium. Therefore, only values measured in a range of $0.1 < z/\delta < 0.5$ were adopted and correlated with Ri. Figure 5 shows a correlation of the ratio of heat and momentum eddy diffusivities, K_h/K_m, with Ri. This is in good agreement with the observational result of Kondo et al. (1978). Thus, similar to the results of Ohya, et al. (1997), turbulence quantities in stable conditions are well correlated with Ri.

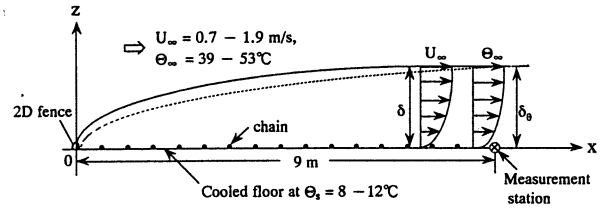

Fig.1. Experimental arrangement (SBL).

Exp. case	N1	S1	S2	S3	S4	S5	S6	S7	S8
U_∞(m s^{-1})	1.76	1.83	1.53	1.29	1.25	1.01	0.81	0.89	0.76
Re_δ	53000	50600	42600	35300	34700	28000	20100	23600	25400
Ri_δ	0	0.12	0.16	0.24	0.27	0.40	0.58	0.67	1.17
δ ($\fallingdotseq \delta_\theta$)(m)	0.45	0.45	0.45	0.45	0.45	0.45	0.40	0.40	0.50
$\triangle\Theta$ (℃)	0	27.4	26.6	27.4	29.4	28.7	30.0	44.0	44.1
u_*/U_∞	0.054	0.043	0.041	0.035	0.030	0.025	0.024	0.018	0.022
$\theta_*/\triangle\Theta$	0	0.030	0.032	0.036	0.032	0.041	0.048	0.033	0.037
u_*(m s^{-1})	0.095	0.078	0.063	0.044	0.038	0.023	0.019	0.016	0.016
θ_*(℃)	0	0.82	0.85	0.98	0.95	1.19	1.46	1.45	1.65
Q_s(℃ m s^{-1})	0	-0.064	-0.053	-0.043	-0.036	-0.027	-0.028	-0.023	-0.027
L (m)	∞	0.557	0.346	0.149	0.115	0.032	0.019	—	—
Symbol	●	×	⊞	⊠	□	◇	▽	△	○

Table1. Experimental data (SBL).

Cal. case	Re_δ	Re_τ	Ri_δ	δ (m)	u_* (ms^{-1})	U_∞(ms^{-1})	Symbol
N	5450	270	0	0.5	0.054	1.09	●
S	5450	160	0.7	0.5	0.032	1.09	○

Table2. Computational data (SBL).

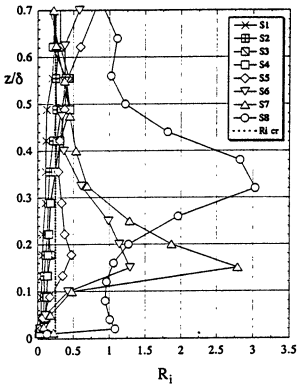

Fig.4. Vertical profiles of gradient Ri number (Exp.).

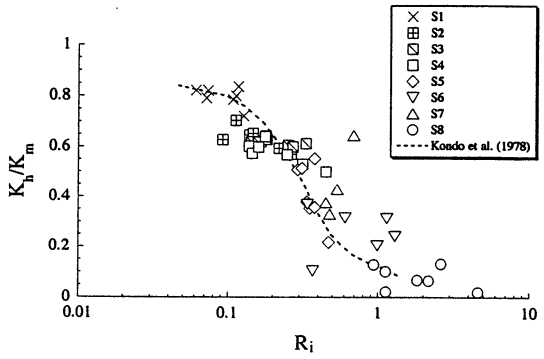

Fig.5. Correlation of Kh/Km with Ri (Exp.).

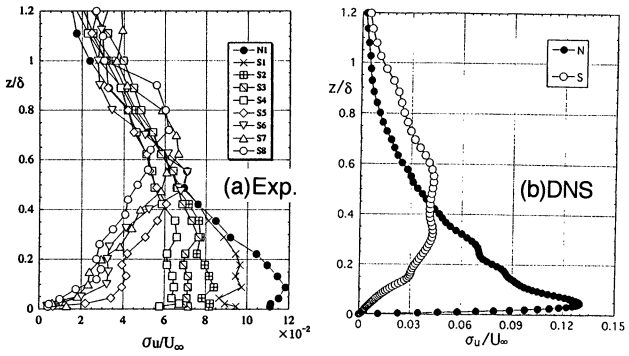

Fig.2. Vertical profiles of u- fluctuation.

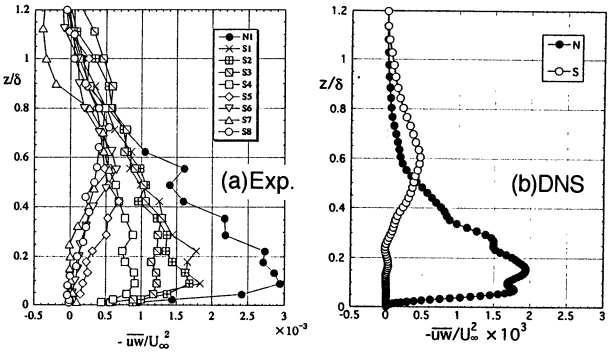

Fig.3. Vertical profiles of $\overline{uw}$ flux.

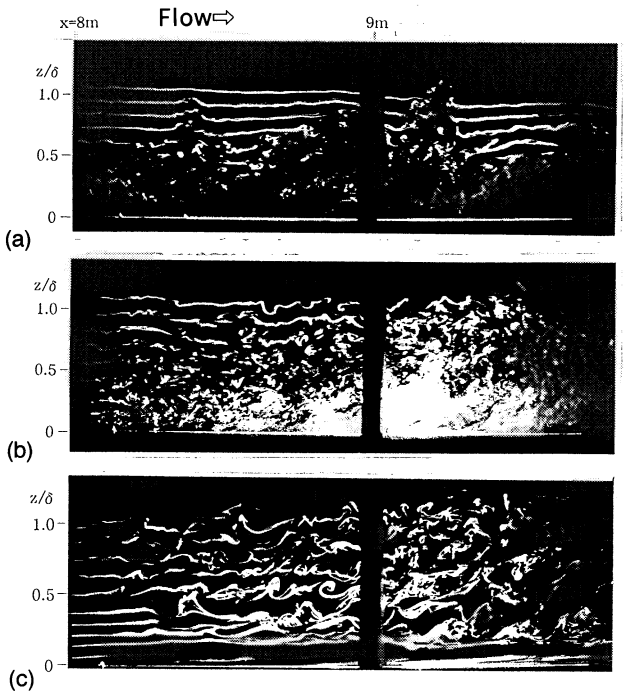

Fig.6. Flow visualization of SBL. Side view of x=8-10m. Flow is left to right. (a) Neutral flow, (b) Stratified flow (Case S2), (c)Stratified flow (Case S8).

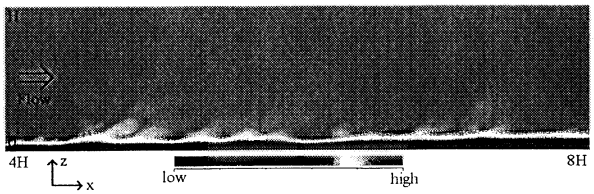

Fig.7. Flow visualization of SBL by DNS. Side view of instantaneous temperature field of x=4 - 8H.

Figure 6 shows the results of the flow visualization experiments by smoke-wire method. A turbulent boundary layer similar to a neutral flow case (Figure 6a) is observed in a stratified flow with weak stability case S2, as seen in Figure 6b. Although the fluctuations of velocity and temperature become weaker with increasing stability, the SBL flows with weak stability seem to be basically similar to a neutral turbulent boundary layer for the vertical structures and turbulent transport processes, as seen in Figures 6a and 6b. On the other hand, wave-like motions driven by buoyancy and waves due to the Kelvin-Helmholtz instability can be observed in a stratified boundary layer with strong stability case S8, as shown in Figure 6c. Figure 7 shows a flow visualization result of strongly stable stratified flow by DNS. The instantaneous temperature field clearly shows wavy motions in the lower part, which are very similar to those of wind tunnel experiments. The almost zero values of momentum and heat fluxes near the ground, as shown in Figure 3, are due to dominant wavy motions in strongly stable stratified flows.

CONVECTIVE BOUNDARY LAYERS

Experimental and Computational Setup

Experiments on simulating the atmospheric convective boundary layer (CBL), capped by a strong temperature inversion and affected by surface shear, are also carried out, as shown in Figure 8. To create a typical CBL in the test section, the floor panels were heated with a surface temperature of around 75℃ and a vertical temperature profile in the entrance of the test section was set as a preshaping profile of CBL with an ambient temperature (around 12℃) from floor to a certain height, 5 ℃/cm in the range of an inversion layer height and 0.33℃/cm in the upper part. The freestream velocities of CBL simulated were U_∞=1.0-1.5m/s and these cover a range of stability from weakly to strongly unstable.

A quasi-stationary, horizontally evolving CBL is reproduced in the test section, with two overall Richardson numbers, as summarized in Table 3. One is $Ri_b(= (g/\Theta_o) \cdot (\Theta_m - \Theta_s) z_i / U_m^2)$ up to -0.74, here, U_m and Θ_m are the mean velocity and temperature in the range where both values show almost constant in the middle part of CBL, Θ_o, the average absolute temperature over the whole CBL depth, Θ_s, the temperature of heated floor, and z_i, the inversion height. The other is $Ri_t (= (g/\Theta_t) \cdot (\Delta\Theta)_t z_i / w_*^2)$ in the inversion layer aloft up to 27.2, here, $(\Delta\Theta)_t$ and Θ_t are the temperature difference and the average absolute temperature over the inversion layer. The shear/buoyancy dynamic ratio u_*/w_* is in the range of 0.3-0.5, here, u_* is the friction velocity and w_* is the convective velocity scale, defined as $(gQ_s z_i/\Theta_o)^{1/3}$, Q_s is the surface kinematic heat flux. The Re $(=U_m z_i/\nu)$, based on the inversion height z_i, ranges from 1.8×10^4 to 2.5×10^4. Measurements of turbulence quantities in the vertical direction were made at a distance of 6 m downstream from the 2D block. Table 4 shows the computational data for CBL. The Reynolds number as well as SBL calculations is much lower than those of experiments.

Results

Table 3 shows the flow conditions for each experimental case (S1 - S3). The vertical profiles in Figures 9 and 10 are normalized by U_m, $\Theta_s - \Theta_m$, w_*, and θ_* (a temperature scale defined as Q_s/w_*), and shown with the normalized height z/z_i.

Figure 9a shows the mean temperature profiles from both wind tunnel experiment and DNS. We can find a range of z/z_i = 0.2 - 0.7 in the profiles where the mean temperatures show an almost uniform value of Θ_m, this is due to a vigorous convective mixing. A large temperature gradient showing a strong inversion layer formed is seen in the upper part of temperature profiles in Figure 9a.

Figures 9b and 9c show the vertical profiles of normalized variances of u and θ. The comparison of the wind tunnel data and DNS results with those of atmospheric and water tank studies of CBL (Figure 10) shows the crucial dependence of the turbulence statistics in the upper part of the layer on the strength of inversion layer, as well as the modification of the CBL turbulence regime by the surface shear. As seen in Figure 9c, a maximum of temperature fluctuation in the inversion layer is successfully simulated in both experiments and DNS. Moreover, a range of negative heat flux in the inversion layer can also be simulated both in wind tunnel experiments and in DNS, as shown in Figure 9d, and is compared with the results of field studies (Figure 10). Thus, a maximum of temperature fluctuation and a range of negative heat flux are due to the large temperature gradient in the inversion layer.

Through the flow visualization experiment, we can observe a number of plumes impinging into the inversion layer as well as the entrainment of the fresh air aloft into the mixed layer, as seen in Figure 11. Furthermore, we can observe a wave-like motion due to interfacial waves in the inversion layer. Figure 12 also shows the instantaneous temperature field of CBL by DNS. We can clearly observe many plumes from the ground and wavy motions in the inversion layer in both side and rear views.

CONCLUSIONS

A thermally stratified wind tunnel is a very useful facility to simulate the atmospheric SBL and CBL in the test section. By using it, we have successfully simulated various vertical profiles of turbulence statistics similar to those from observed SBL and CBL in the field studies. DNS for SBL and CBL with similar boundary conditions to experimental ones have also been conducted. Some interesting features for both

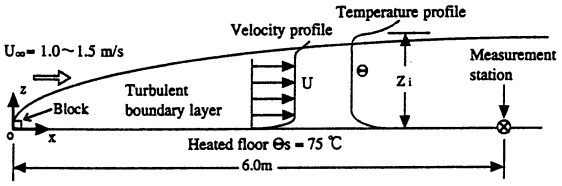

Fig.8. Experimental arrangement (CBL).

Cal. case	Re	Re_τ	Ri_b	z_i(m)	w_*(ms^{-1})	U_m(ms^{-1})	Symbol
S	2400	226	-0.41	0.29	0.125	0.82	-○-

Table4. Computational data (CBL).

Exp. Case	S1	S2	S3
Symbol	○	△	□
U_m [m/s]	1.34	1.04	0.86
$\Delta\Theta=\Theta_m-\Theta_s$ [K]	-53.9	-52.6	-52.8
z_i [m]	0.28	0.28	0.32
w_* [m/s]	0.13	0.12	0.11
θ_* [K]	1.80	1.50	1.17
u_*/w_*	0.50	0.36	0.30
Ri_b	-0.28	-0.45	-0.74
Ri_t	11.19	16.31	27.24
Re	25000	19400	18400

Table3. Experimental data (CBL).

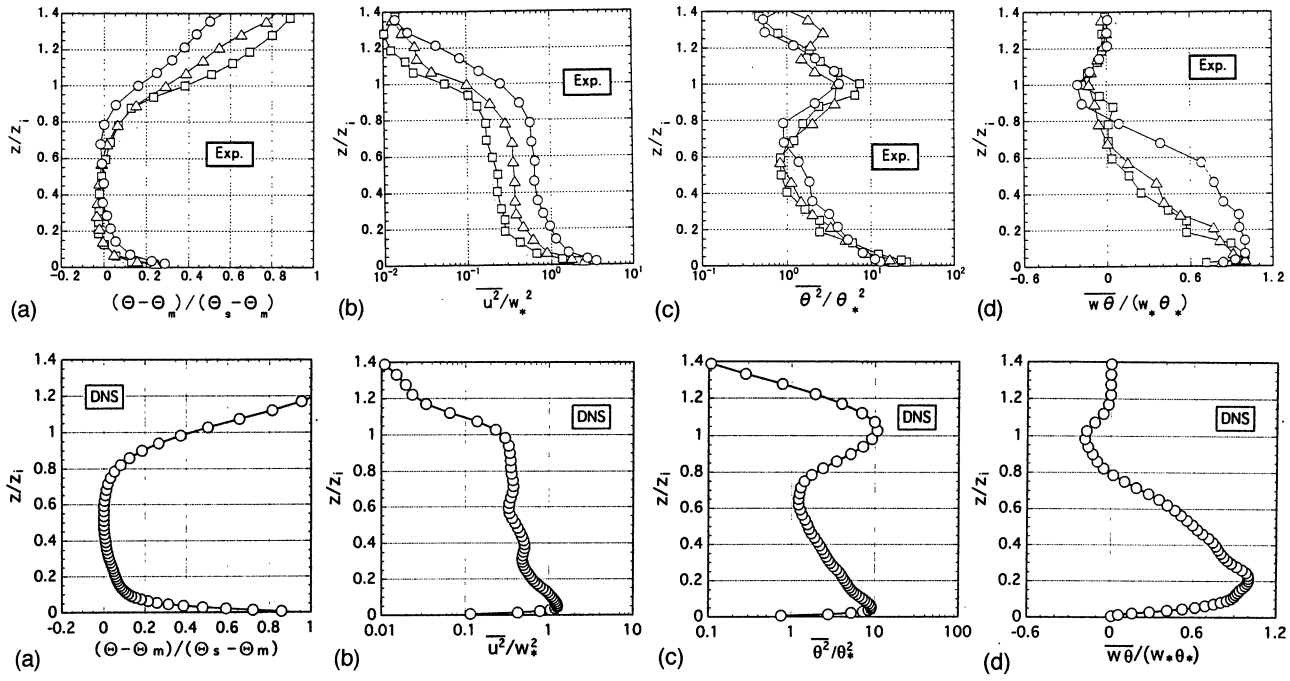

Fig.9. Vertical profiles of mean temperature, u and θ variances, and $\overline{w\theta}$ flux. Upper, Exp. ; Lower, DNS.

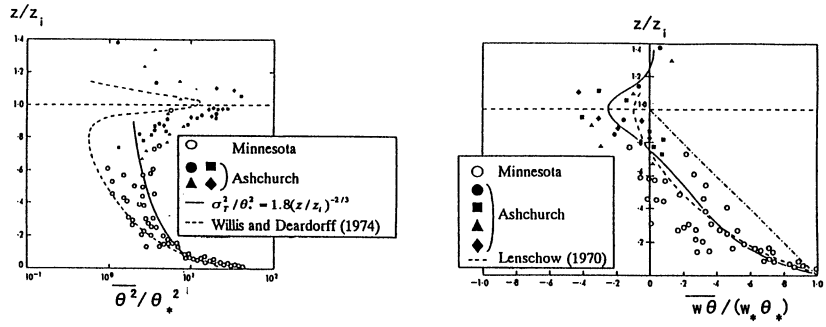

Fig.10. Profiles of θ variance and $\overline{w\theta}$ flux (Observation, after Caughey 1984).

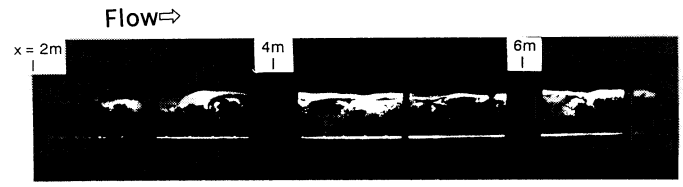

Fig.11. Flow visualization of CBL for case S3. Flow is left to right. Smoke is generated at the inversion height.

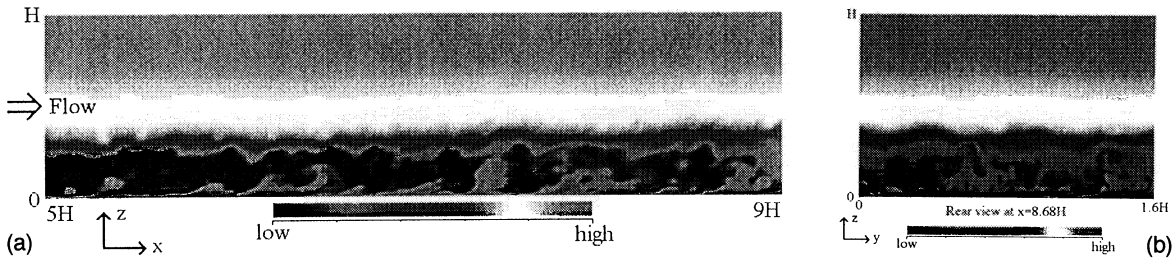

Fig.12. Instantaneous temperature field of CBL by DNS. (a) Side view of x=5-9H, (b) Rear view at x=8.7H

SBL and CBL could be obtained as follows.

For SBL experiments, the vertical profiles of turbulence statistics exhibit different behavior in two distinct stability regimes of the stratified flows with weak and strong stability, corresponding to the vertical profiles of the local Richardson number. Wave-like motions driven by buoyancy and waves due to the Kelvin-Helmholtz instability were observed in stratified boundary layers with strong stability.

For CBL experiments, a maximum of temperature fluctuation and a range of negative vertical heat flux in the inversion layer could clearly be simulated in the present wind tunnel experiment. A number of plumes impinging into the inversion layer as well as the entrainment of the fresh air aloft into the mixed layer were observed. It should be noted that the negative heat flux in the inversion layer are attributed to both of impinging of plumes and the entrainment of the upper air. The results obtained in wind tunnel experiments could almost be reproduced in DNS. This means the mutual accuracy and reliability both in wind tunnel experiments and DNS.

REFERENCES

Arya, S.P.S., 1975, "Buoyancy Effects in a Horizontal Flat-Plate Boundry Layer," J. Fluid Mech. 68 (2), pp.321-343.

Arya, S.P.S., 1982, "Atmospheric Boundary Layers Over Homogeneous Terrain,", Engineering Meteorology, E. Plate(edi), Elsevier, pp.237-267.

Caughey, S.J., J.C.Wyngaard and J.C.Kaimal, 1979, "Turbulence in the Evolving Stable Boundary Layer," J. Atmos. Sci. 36, pp.1041-1052.

Caughey, S.J., 1984, "Observed Characteristics of the Atomospheric Boundary Layer," in F.T.M. Nieuwstadt and H. van Dop (eds.), Atmospheric Turbulence and Air Pollution Modelling. D. Reidel Pub. Co., pp.107- 158.

Fedorovich, E., R. Kaiser, M. Rau and E. Plate, 1996, "Wind tunnel study of turbulent flow structure in the convective boundary layer capped by a temperature inversion," J.of the Atmos. Sci., 53 (9), pp.1273-1289.

Komori, S., H. Ueda, F. Ogino and T. Mizushima, 1983, "Turbulence Structure in Stably Stratified Open-channel Flow," J. Fluid Mech. 130, pp.13-26.

Kondo, J., O. Kanechika and N. Yasuda, 1978, "Heat and Momentum Transfers under Strong Stability in the Atmospheric Surface Layer," J. Atmos. Sci. 35, pp.1012-1021.

Mahrt, L., J. Sun, W. Blumen, T. Delany and S. Oncley, 1998, "Nocturnal Boundary-Layer Regime. Boundary- Layer Meteorol.," 88 (2), pp.255-278.

Mahrt, L., 1999, "Stratified Atmospheric Boundary Layers," Boundary-Layer Meteorol., to appear.

Meroney, R.N. and W.H. Melbourne, 1992, "Operating Ranges of Meteorological Wind Tunnels for the Simulation of Convective Boundary Layer (CBL) Phenomena," Boundary-Layer Meteorol., 61, pp.145- 174.

Nieuwstadt, F.T.M., 1984, "The Turbulent Structure of the Stable Nocturnal Boundary Layer," J. Atmos. Sci. 41, pp.2202-2216.

Ohya, Y., M. Tatuno, Y. Nakamura, and H. Ueda, 1996, "A thermally stratified wind tunnel for environmental flow studies," Atmos. Environ., 30 (16), pp.2881-2887.

Ohya, Y., D.E. Neff and R.N. Meroney, 1997, "Turbulence structure in a stratified boundary layer under stable conditions," Boundary-Layer Meteorol. 83, pp.139-161.

Stull, R.B., 1988, "An Introduction to Boundary Layer Meteorology," Kluwer Academic Publishers, pp.499-513.

Willis, G.E. and J.W. Deardorff, 1974, "A Laboratory Model of the Unstable Planetary Boundary Layer," J. Atmos. Sci. 31, pp.1297-1307.

Wyngaard, J.C., 1992, "Atmospheric Turbulence," Annu. Rev. Fluid Mech. 24, pp.205-233.